Spin Trapping of Oxygen-centred Radicals by Substituted *N*-Benzylidene-*tert*-butylamine *N*-Oxides

Yukino Abe, Shin-ya Seno, Kazuhisa Sakakibara * and Minoru Hirota
Department of Synthetic Chemistry, Faculty of Engineering, Yokohama National University, Hodogaya-ku, Yokohama 240, Japan

Spin-trapping of oxygen-centred radicals (*tert*-butoxyl and carboxyl) by substituted *N*-benzylidene-*tert*-butylamine *N*-oxides (X-PBN) has been studied and the rates have been measured by means of EPR experiments. The experimental results revealed a substituent effect [X-PBN with an electron-donating substituent favours spin trapping ($\rho < 0$)] and are rationalized by an electron-transfer mechanism between the frontier orbitals of the reactants. The reaction pathway has been deduced from molecular-orbital and molecular-mechanics calculations.

The spin-trapping[1] technique is a useful tool, enabling chemists to detect short-lived radicals easily with the usual EPR instruments. However, the identification of spin adducts by EPR spectroscopy is rather difficult because the variation of the hyperfine constants of spin adducts (a_N and a_H^β) due to the structural changes of the trapped radicals is not very large. Therefore the application of spin trapping to complex systems, where several active radicals coexist, has been limited.

The combination of separation techniques and other analytical methods (HPLC[2] and GLC–MS[3] *etc.*) with spin trapping has made this technique more powerful and widely applicable. As well as the improvement of spin-trapping methods by coupling with other analytical methods, a new spin trapping technique[4] using ^{13}C labelled spin-trapping reagents has been developed in order to identify spin adducts clearly. In order to improve the applicability of the spin-trapping method further, more information must be obtained on the reaction mechanism and on the selectivity of spin traps towards radical species.

In our previous report,[5] we investigated the relative rates of the spin-trapping reactions of substituted *N*-benzylidene-*tert*-butylamine *N*-oxides (X-PBN; abbreviated after its common name phenyl *tert*-butyl nitrone) with substituted phenyl radicals ($YC_6H_4^\bullet$) and found that aryl free radicals having an electron-donating substituent were readily captured by electron-deficient spin traps, and *vice versa*. In this paper, we have studied the spin-trapping reactions of oxygen-centred radicals (*tert*-butoxyl, carboxyl) with X-PBN in order to elucidate how selectively radical species can be captured by proper spin traps, and how effectively spin adducts can be identified. The steric course of the approach of the free radical towards the spin trap, as well as the electronic and steric effects of substituents on the spin-trapping reaction, are also intriguing aspects. These were investigated by estimating the structures of transition states and products with the aid of molecular-orbital and molecular-mechanics calculations.

Results and Discussion

Spectra of Spin Adducts of Oxygen-centred Radicals.—*tert*-Butoxyl radical was generated by the thermal decomposition of di-*tert*-butyl peroxyoxalate (DBPO; **1**). Carboxyl radicals ($RCO_2^\bullet$) were also generated by the thermal decomposition of *N*-(acyloxy)pyridine-2-thione (**2**).[6]

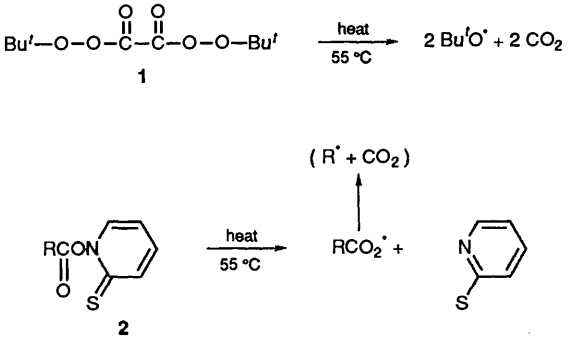

EPR spectra of the spin adducts produced from the above systems showed a typical triplet of doublets splitting pattern, characteristic of aminoxyl radicals. Other peaks could also be observed at the lowest and highest magnetic field regions in the spectra of carboxyl ($RCO_2^\bullet$) spin adducts of X-PBN in the case where R is phenyl or cyclohexyl. The intensity of these additional peaks was rather low in the case of cyclohexanecarboxyl while they could easily be detected, with fairly high intensity, in the case of benzoyloxyl trapping. They could be assigned to alkyl spin adducts by comparing the EPR spectrum with that of an authentic sample and by GLC–MS analysis of the phenyl spin adduct of PBN. In the case of the cyclohexanecarboxyl trapping by X-PBN, the intensity of the peaks of cyclohexyl adducts increased as the substituent (X) became more electronegative. In Table 1, observed a_N and a_H^β values of spin adducts of these oxygen-centred radicals are shown together with the data for alkyl and aryl spin adducts. The nitrogen hyperfine splitting constants (a_N) reflect the electronic properties of the captured radicals, but are insensitive to their structure. The a_N values of spin adducts of oxygen-centred radicals are smaller (13.3–14.0 G) than those of carbon-centred radicals (14.3–14.9 G). The smaller values of a_N can be ascribed to the higher electronegativity of captured oxygen-centred radicals. The RO or RCO_2 moiety in the spin adduct reduces electron density around the aminoxyl function and causes the a_N values to decrease. Doublet splitting constants (a_H^β) and *g*-values were perturbed by the electronegativity effect to a considerably lesser extent than a_N.

N-Benzylidene[$^2H_5$]aniline *N*-oxide ([$^2H_5$]DPN;[6] **5**) is a nitrone which has an EPR spectrum distinguishable from those of X-PBN spin adducts. As shown in Table 1, a_N values of [$^2H_5$]DPN spin adducts are smaller (10.7, 10.9 G) than those of X-PBN spin adducts. This is due to the resonance effect of the phenyl ring adjacent to the aminoxyl group. The decrease in the spin density on the N atom of the aminoxyl function due to delocalization into the phenyl ring leads to a smaller a_N value. The a_H^β value of the [$^2H_5$]DPN spin adduct of *tert*-butoxyl radical is larger (4.0 G) than those of other spin adducts. This is

partly due to the change in the structure of spin adducts. In the case of the [$^2H_5$]DPN spin adduct of *tert*-butoxyl radical, steric hindrance between *tert*-butoxyl and phenyl groups decreases the dihedral angle formed by the π-orbital of the aminoxyl nitrogen atom and the β-hydrogen which, in turn, makes a_H^β large. EPR spectra of X-PBN spin adducts are useful in determining whether the trapped radical is oxygen-centred or carbon-centred. However, spin adducts could not be identified unequivocally by a_N and a_H^β values. Thus EPR spectroscopy becomes more effective when used in combination with other analytical techniques.

GLC–MS Analyses of Spin Adducts.—We carried out GLC–MS measurements of the PBN spin adducts of oxygen-centred radicals in order to identify them clearly. As spin adducts are not stable enough to survive the process of GLC separation, spin adducts were trimethylsilylated so as to increase their thermal stability and volatility. The results are shown in Table 2. These trimethylsilylated spin adducts showed the characteristic fragment ion peaks which have been reported in the mass spectra of trimethylsilylated PBN aryl spin adducts.[3] The M − 15 [M − CH_3], M − 58 [M − Bu^t − H], M − 73 [M − $Si(CH_3)_3$ or M − Bu^t − CH_3 − H] peaks gave clear evidence of the existence of *tert*-butoxyl, benzoyloxyl and cyclohexanecarboxyl spin adducts. GLC–MS analyses of trimethylsilylated spin adducts can identify the captured radicals without ambiguity.

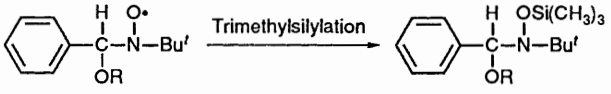

Table 1 Hyperfine splitting constants a_N and a_H^β for (*a*) oxygen-centred spin adducts with X-PBN, and (*b*) carbon- and oxygen-centred spin adducts with PBN

(*a*)	Radical					
	Bu^{t}O$^\bullet$		*cyclo*-$C_6H_{11}CO_2^\bullet$		$PhCO_2^\bullet$	
Spin trap	a_N	a_H^β	a_N	a_H^β	a_N	a_H^β
X-PBN						
X = *p*-CH_3	13.8	2.1	14.0	1.9	13.4	1.5
m-CH_3	13.8	2.1	14.0	1.9	13.5	1.5
H	13.8	2.2	13.9	1.9	13.3	1.5
m-CH_3O	14.0	2.3	13.9	1.9	13.8	1.6
p-Cl	13.9	2.3	13.3	1.8	13.5	1.4
m-Cl	13.7	2.0	13.6	1.9	13.4	1.5
m-CN	14.1	2.2	14.1	1.8	13.5	1.5
p-CN	14.0	2.0	14.2	1.9	13.3	1.5
m-NO_2	13.9	1.9	13.3	1.8	13.2	1.5
p-NO_2	13.5	2.4	13.5	1.9	13.2	1.5
o-CH_3	13.3	2.4	12.8	2.4	14.0	3.0
o-Cl	13.7	2.5	12.7	2.7	13.7	2.1
[$^2H_5$]DPN	10.7	4.0	10.9	2.9		

(*b*)	Radical			
	$RCO_2^\bullet$		$R^\bullet$	
R	a_N	a_H^β	a_N	a_H^β
CH_3	13.3	2.1	14.9	3.5
C_2H_5	13.4	2.0	14.3	3.3
iso-C_3H_7	13.8	1.9	14.7	2.6
tert-C_4H_9	13.9	1.9	14.7	2.3

Relative Rates of Spin-trapping Reactions of Substituted N-*Benzylidene*-tert-*butylamine* N-*oxides* (*X-PBN*) *with* tert-*Butoxyl or Carboxyl Radicals.*—The relative reactivities of X-PBN's towards *tert*-butoxyl or carboxyl radicals were determined by competitive reactions using [$^2H_5$]DPN (**5**) as a reference.

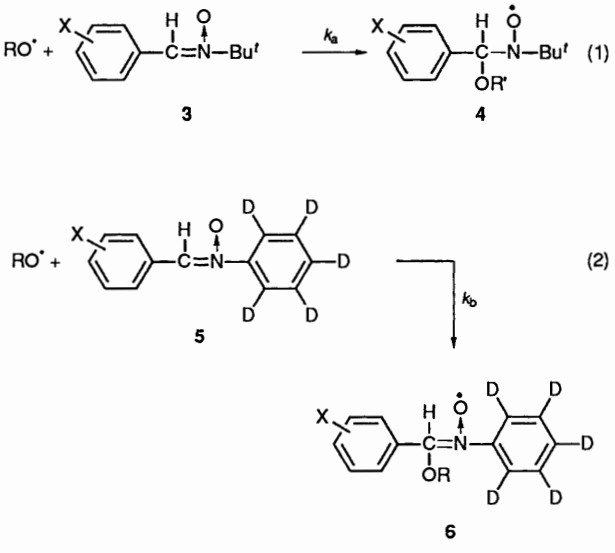

Table 3 Relative rate constants (k_X/k_H) of the spin trapping reactions of oxygen-centred radicals with X-PBNs

Spin trap X-PBN	Radical	
	Bu^{t}O$^\bullet$	*cyclo*-$C_6H_{11}CO_2^\bullet$
X = *p*-CH_3	1.25	1.25
m-CH_3	1.10	1.08
H	1.00	1.00
m-CH_3O	0.98	0.90
p-Cl	0.86	0.78
m-Cl	0.84	0.67
m-CN	0.78	0.39
p-CN	0.66	0.24
m-NO_2	0.65	0.17
p-NO_2	0.62	0.13
o-CH_3	0.73	—
o-Cl	0.71	—

Table 2 GLC–MS of the trimethylsilylated adducts of PBN with oxygen-centred radicals.

Radical	t_R/min[a]	Fragmentation [Relative intensity (%)]				
		M	[M − 15]	[M − 58]	[M − 73]	73
Bu^{t}O$^\bullet$	11.2	323	28	55	100	80
cyclo-$C_6H_{11}CO_2^\bullet$	9.5	377	1	14	87	100
$PhCO_2^\bullet$	6.5	371	6	11	43	10

[a] Retention time.

As X-PBN spin adducts have considerably different a_N values from those of DPN adducts (Table 1), relative concentrations of the spin adducts formed can be determined from EPR spectra of the competing reactions. The use of [$^2H_5$]DPN instead of unlabelled DPN has the advantage of eliminating undesirable overlapping of the hyperfine splitting lines caused by phenyl. The relative rate constant (k_a/k_b) can be expressed in terms of the relative rates for generating spin adducts at an early stage of the reaction and the initial concentrations of the competing spin-trapping reagents as given in eqn. (3) The relative rate, in turn, can be estimated as the concentration ratio of produced spin adducts **4** and **6** at an early stage.

$$\frac{k_a}{k_b} = \frac{[\text{DPN}](\text{d}[\mathbf{4}]/\text{d}t)_{t\to 0}}{[\text{X-PBN}](\text{d}[\mathbf{6}]/\text{d}t)_{t\to 0}} \qquad (3)$$

Relative rates of tert-*butoxyl radical trapping by X-PBN.* In order to investigate the electronic effect of *meta-* and *para-*substituents, relative rates (k_X/k_H) were determined by means of EPR experiments and are given in Table 3. The *meta-* and *para-*substituted X-PBNs with electron-donating substituents could trap *tert*-butoxyl radical smoothly, as found in the spin trapping of electron deficient aryl radicals by X-PBN. *ortho-*Substituents reduced the rates of spin trapping irrespective of their electronic nature. This sort of *ortho*-effect was also observed in the trapping reactions of aryl radicals, and attributed to their steric hindrance. The relative rates (k_X/k_H) (normalized to the rate of reaction of PBN with *tert*-butoxyl radical) were plotted against Hammett σ constants[8] (Fig. 1). The reaction constant 2ρ was found to be -0.29 from the slope (correlation coefficient, $r = 0.985$). Although the substituent effect is not very large, this result indicates that electron transfer from X-PBN to *tert*-butoxyl radical in the transition state facilitates the spin trapping reaction. It is quite natural that the reaction constant ρ for *tert*-butoxyl radical trapping (-0.29) has a larger negative value than that for phenyl radical trapping (-0.18) because the *tert*-butoxyl radical is more electronegative than the phenyl radical.

Relative rates of carboxyl radical ($RCO_2^{\bullet}$) *trapping by X-PBN.* The reaction constant ρ for the benzoyloxyl radical trapping by X-PBN was reported to be -0.47 by Sommermeyer's group.[9] The Hammett plot for the cyclohexanecarboxyl radical trapping reactions by X-PBNs showed an irregular substituent effect (Fig. 1). The relative rate (k_X/k_H) decreased linearly as the substituent X changed from an electron-donating *p*-CH_3 to electron-withdrawing *m*-Cl. However the Hammett plot gradually deviated from this line as substituent X became more electronegative (*m*-, *p*-CH or NO_2). The deviation from the linear Hammett plot was due to the decarboxylation proceeding competitively with the spin trapping reaction. This was confirmed by detection of the cyclohexyl adduct of the X-PBN by EPR spectroscropy. From the linear part of the Hammett plot, the reaction constant ρ was estimated to be -0.49. The ρ value was as large as that for benzoyloxyl trapping. The ρ value can be accounted for by electron transfer from X-PBN to cyclohexanecarboxyl which stabilizes the transition state and facilitates the spin trapping reactions. The side reaction forming cyclohexyl adducts of X-PBN was noticeable in the case when substituent X was strongly electron-withdrawing. This fact can be explained by electron transfer from the cyclohexyl radical to X-PBN in the transition state. As the cyclohexyl radical tends towards having electropositive character (carbocation), the process involving electron transfer from cyclohexyl radical to X-PBN becomes energetically favourable. This process should be more favourable when X is more electronegative. Therefore, considerable amounts of the cyclohexyl adducts of X-PBNs could be detected when X was a strong electron-withdrawing group.

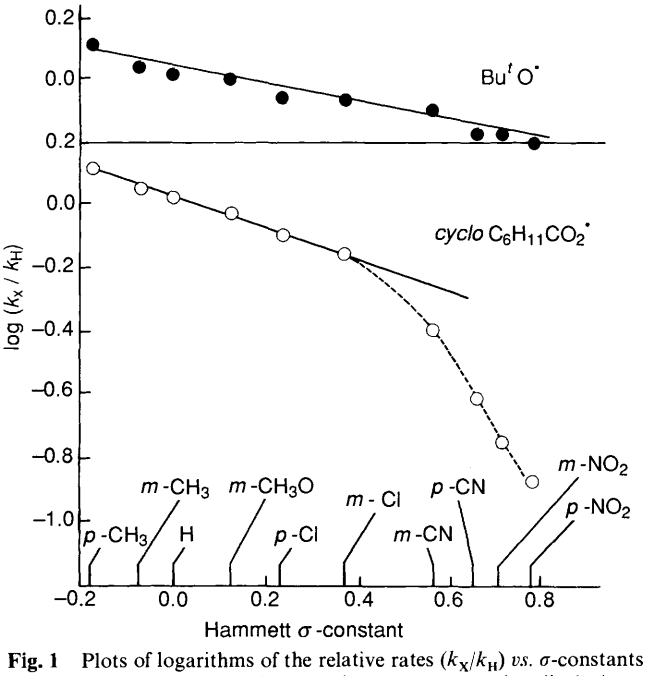

Fig. 1 Plots of logarithms of the relative rates (k_X/k_H) *vs.* σ-constants of the substituents on X-PBN for the oxygen-centred radicals (*tert*-butoxyl or cyclohexanecarboxyl) spin-trapping reactions

The *ortho*-substituent effect could not be evaluated accurately because the hyperfine constants (a_N, a_H^{β}) of X-PBNs and [$^2H_5$]DPN adducts are quite similar, causing a serious overlap of the peaks of both spin adducts.

Absolute Rate Constants for Carboxyl ($RCO_2^{\bullet}$) *Radical Trapping by X-PBN.*—In the carboxyl-radical spin-trapping experiments where radicals were generated by thermal decomposition of *N*-(acyloxy)pyridine-2-thione (Barton's reagent, **2**), spin adducts of carbon-centred radicals were also detected in addition to the normal carboxyl spin adducts. The spin-trapping reaction in benzene can be expected to proceed through a combination of elementary processes [eqns. (4)–(8)]. In order to investigate the reaction mechanism of this carboxyl radical trapping in detail, the rate constant for every elementary process was determined experimentally.

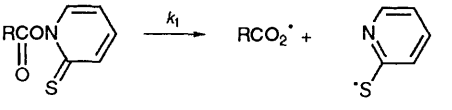

(4)

Barton's reagent (**2**)

$RCO_2^{\bullet}$ + PBN $\xrightarrow{k_2}$ RCO_2-SA (5)

$RCO_2^{\bullet}$ $\xrightarrow{k_3}$ $R^{\bullet}$ + CO_2 (6)

$R^{\bullet}$ + PBN $\xrightarrow{k_4}$ R-SA (7)

$R^{\bullet}$ + C_6H_6 (solvent) $\xrightarrow{k_5}$ Phenylated product (8)

Under the conditions where a large excess of PBN was used relative to the amount of Barton's reagent, and the amount of spin adducts of carbon-centred radicals produced could be expected to be quite small at an early stage of the spin-trapping reaction, the self-trapping reaction by *N*-acyloxypyridine-2-thione could be neglected. Assuming that carbon radical concentration [$R^{\bullet}$] is almost zero at the initial stage, eqn. (9) could be derived from eqns. (4), (5) and (6).

Table 4 Rate constants for each elementary process in the carboxyl radical trapping where radicals were generated by thermal decomposition of *N*-acyloxypyridine-2-thione

Radical	$k_1/10^{-4}$ s^{-1}	k_2/k_3
cyclo-$C_6H_{11}CO_2^{\bullet}$	1.1	29
$PhCO_2^{\bullet}$	1.3	107

$$\frac{[2]}{d[RCO_2\text{-}SA]/dt} = \frac{1}{k_1} + \frac{k_3}{k_1k_2}\frac{1}{[PBN]} \quad (9)$$

The rate constant k_1 and the ratio for k_3/k_2 were determined on the basis of eqn. (9) by measuring the initial rate for the production of carboxyl-radical spin adduct $d[RCO_2\text{-}SA]/dt$ by EPR experiments. The rate constants obtained from the slope and intercept of the plot of eqn. (9) are given in Table 4 and indicate that the decomposition rates of *N*-acyloxypyridine-2-thione (**2**; R = cyclohexyl or phenyl) are *ca.* 10^{-4} s^{-1}. By using the k_2/k_3 value of 107 and the reported decomposition rate constant k_3 (10^4 s^{-1})[10] for the benzoyloxyl radical, the constant k_2 for benzoyloxyl radical trapping by PBN was estimated to be *ca.* 10^6 s^{-1}, which is approximately the same as that reported from experiments in which PBN captured benzoyloxyl radicals generated by the thermal decomposition of benzoyl peroxide.[11] The k_2/k_3 values in Table 4 indicated that the decarboxylation of cyclohexylcarboxyl radical proceeded more rapidly than that of benzoyloxyl radical. This led us to expect that cyclohexyl spin adducts might be easily observed. The EPR experimental results however, showed the adverse tendency for spin adduct formation. That is to say, while phenyl spin adducts were always detected in addition to benzoyloxyl spin adducts, cyclohexyl spin adducts could only be observed with low intensity when X-PBN with an electron-withdrawing substituent was used as a spin trap. This contradiction will be discussed later by considering the results of theoretical calculations.

Theoretical Study of the Spin-trapping Reaction.—Molecular-orbital calculations (AM1[12]) were carried out in order to rationalize the substituent effects theoretically and to obtain information on how the radical approaches the spin trap to form the transition state. As the spin adducts are paramagnetic and the molecular sizes are rather big, exhaustive and elaborate geometry optimization calculations by AM1 to find stable conformers of spin adducts are time-consuming and impractical. For this reason we used molecular mechanics (MM2[13]) calculations to find their approximate stable conformations in a reasonable cpu time. The necessary force-field parameters for aminoxyl molecules have been estimated from the empirical equations previously reported by us.[14] The MM2-optimized structures were then used as the input data for AM1 calculations, and the geometry reoptimizations were carried out to find out the structures and conformational energies. The structure of *tert*-butoxyl radical was estimated by MM2 calculation by use of the reported force field parameter[15] for alkoxyl radicals. The structures for phenyl,[16] cyclohexyl,[17] benzoyloxy[18] and cyclohexanecarboxyl[17] radicals were estimated from the reported data. By using these geometries for the spin traps and the free radicals, AM1 calculations were carried out on the spin-trapping system.

It is generally recognised that the charge-transfer interaction becomes more favourable as the energy difference between interacting molecular orbitals becomes smaller. In the spin-trapping reaction, the interaction between the frontier orbitals of the radical and the spin trap should play a crucial role in its process. The energy of the highest occupied molecular orbital (HOMO) and the lowest unoccupied molecular orbital (LUMO) of radicals and spin traps were calculated by AM1 and the energy differences between the two alternative pairs of HOMO and LUMO were obtained in order to find which of them is the dominant charge-transfer path in the transition state. The results are shown in Table 5.

In the cases of spin trapping of *tert*-butoxyl and carboxyl ($RCO_2^{\bullet}$) radicals which have an electronegative centre, the frontier orbital energy difference between the LUMO of the radical and the HOMO of the spin trap $[E_{LUMO}(R^{\bullet}) - E_{HOMO}(T)]$ is smaller than that between the LUMO of the spin trap and the HOMO of the radical $[E_{LUMO}(T) - E_{HOMO}(R^{\bullet})]$. The energy difference $[E_{LUMO}(R^{\bullet}) - E_{HOMO}(T)]$ becomes smaller as the substituent X on the spin trap becomes more electron-donating. These calculated results predict that charge-transfer from the HOMO of the spin trap to the LUMO of the radical plays an important role in the spin-trapping reaction, and the reaction rate becomes faster as X-PBN becomes more electron-donating. This prediction is consistent with the experimental results.

In contrast, the $[E_{LUMO}(T) - E_{HOMO}(R^{\bullet})]$ value becomes smaller as X becomes more electron-withdrawing in the cases of the spin trapping of R$^{\bullet}$(cyclohexyl) radical by X-PBN, since $[E_{LUMO}(T) - E_{HOMO}(R^{\bullet})]$ is smaller than $[E_{LUMO}(R^{\bullet}) - E_{HOMO}(T)]$. This is in line with the EPR experimental result showing that a small amount of cyclohexyl spin adduct could be observed together with the major cyclohexanecarboxyl spin adduct when the substituent X was strongly electron-withdrawing. The carbon-centred radicals can be assumed to be more electropositive than the reactive site of PBN. Thus the spin trapping of carbon-centred radical by X-PBN proceeds more favourably as X becomes more electron-withdrawing because the charge-transfer interaction from the HOMO of the radical to the LUMO of the spin trap is energetically more favourable. As the above-mentioned electron-transfer mechanism correctly predicted the relative rate of the spin trapping of aryl radicals by X-PBNs,[5] this mechanism can be extended to the qualitative prediction of the spin-trapping reactions.

Though the electronic substituent effect on the spin trapping could be estimated from the energy levels of frontier orbitals of spin traps and radicals, the problem of the steric effect still remains unsolved. The steric course of the reaction and the structure of the transition state need further investigation. *ab initio*-Transition state calculation is theoretically a proper method of obtaining information about the transition state. Its execution seems impractical because the reaction system is too large for the sophisticated calculation. Therefore we assumed a quasi-transition state, which was estimated by MM2 and AM1 calculations. In the case of *tert*-butoxyl radical trapping, the preliminary MM2 geometry optimization calculations, where the distance between the oxygen atom of the *tert*-butoxyl radical and the nitrone carbon was fixed at several given values (r_x) and other geometrical parameters were optimized, indicated that the system became energetically most favourable at r_x = 1.90 Å. The probable paths of approach were estimated from these MM2 calculations and are shown in Fig. 2.

As the steric energies from MM2 of the two possible quasi-transition states are almost the same, these two paths might be expected to occur with nearly equal probability. In the cases of the spin-trapping reactions of *ortho*-substituted X-PBNs, energy barriers for passing through these transition states would be varied. *ortho*-Substituted X-PBNs adopt a stable conformation in which the phenyl ring and the C=N bond are not coplanar. In order to minimize the steric repulsion between the *ortho*-substituent and other groups on the nitrone moiety, the *ortho*-substituent tends to be located adjacent to the α hydrogen. If we assume that the *tert*-butoxyl radical approaches the spin traps as shown in Fig. 2, the *ortho*-substituent in X-PBN may block the access of the *tert*-butoxyl radical which

Table 5 The frontier orbital energy differences (eV) between X-PBNs and radicals

Radical	Electron transfer process[a]	X: *p*-CH_3	H	*p*-NO_2
$Bu^tO^{\bullet}$	$E_{LU}(T) - E_{HO}(R)$	8.45	8.44	7.36
	$E_{LU}(R) - E_{HO}(T)$[b]	7.53	7.65	8.33
$PhCO_2^{\bullet}$	$E_{LU}(T) - E_{HO}(R)$	10.19	10.19	9.10
	$E_{LU}(R) - E_{HO}(T)$[b]	6.43	6.54	7.22
cyclo-$C_6H_{11}CO_2^{\bullet}$	$E_{LU}(T) - E_{HO}(R)$	11.06	11.06	9.97
	$E_{LU}(R) - E_{HO}(T)$[b]	6.42	6.53	7.22
$Ph^{\bullet}$	$E_{LU}(T) - E_{HO}(R)$	9.86	9.86	8.77
	$E_{LU}(R) - E_{HO}(T)$[b]	8.67	8.78	9.47
cyclo-$C_6H_{11}^{\bullet}$	$E_{LU}(T) - E_{HO}(R)$[b]	8.65	8.65	7.56
	$E_{LU}(R) - E_{HO}(T)$	9.44	9.56	10.24

[a] $E_{LU}(T) - E_{HO}(R)$ indicates the frontier orbital energy difference (eV) between the LUMO of the spin trap and the HOMO of the radical. [b] Energetically favourable electron transfer process.

Table 6 Structural and energy changes of the PBN and $Bu^tO^{\bullet}$ system during spin adduct formation[a]

r_x(2–3)/Å	r(1–2)/Å	θ(1–2–3)/°	ω(1–2–6–7)/°	ω(6–2–1–5)/°	ω(3–2–1–5)/°	ω(1–2–3–4)/°	ΔE/eV
—	1.322	126.9	−0.9	−179.9	—	—	—
2.20	1.378	123.5	−24.8	−160.3	92.8	−135.9	1.464
2.05	1.399	122.8	−33.5	−164.9	82.5	−165.5	1.469
2.00	1.406	120.7	−45.6	−153.1	98.1	−148.4	1.474
1.90	1.420	117.3	−52.0	−146.9	101.9	−140.7	1.322
1.42	1.506	110.8	−75.2	174.0	53.3	−148.8	0.000

[a] Numbering is as in Fig. 2.

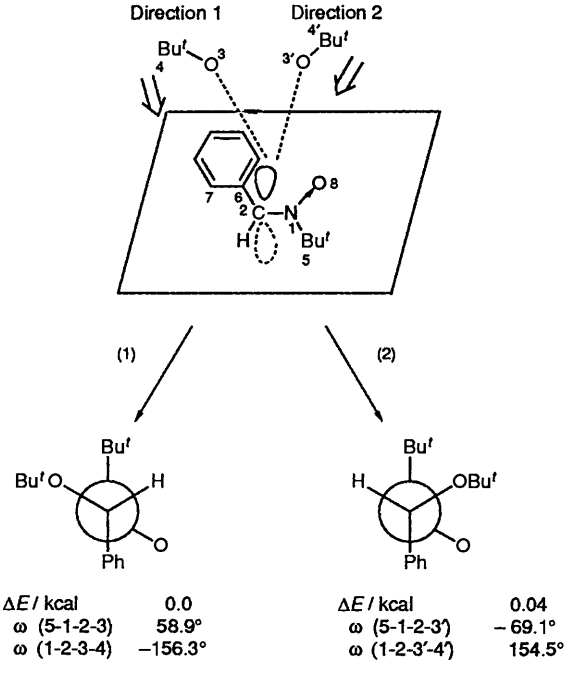

Fig. 2 Probable paths of approach for the spin trapping reaction between PBN and *tert*-butoxyl radical

comes from direction (1) and will lead to the retardation of the spin trapping reaction. Although the MM2 calculations for the quasi-transition state of spin trapping are qualitative and approximate, the decrease in reactivity for *ortho*-substituted X-PBNs can reasonably be explained.

In order to obtain further information about the transition state for the *tert*-butoxyl spin-trapping reaction, AM1 calculations were carried out. The distance (r_x) between *tert*-butoxyl oxygen atom and nitrone carbon was selected as the reaction co-ordinate and r_x was varied in the range of 1.40–2.20 Å. Other geometrical parameters were optimized by UHF AM1 calculations by using the MM2 optimized geometries as the initial data. The geometry, energy, spin density and charge of the *tert*-butoxyl radical–X-PBN system are listed as functions of r_x in Table 6, Fig. 3 and Fig. 4, respectively. As the *tert*-butoxyl radical approaches PBN, the conformation of nitrone nitrogen atom gradually changes from planar to pyramidal. At r_x = *ca.* 2.0 Å, the energy has a maximum value. At the initial stage of spin-trapping reaction ($r_x \approx 2.5$ Å), β spin is induced on the nitrone carbon (C-2) due to the localization of α spin on the *tert*-butoxyl oxygen. As the reaction proceeds, the spin polarization decreases and the spin gradually becomes concentrated on the aminoxyl group. The change in electron density may explain the electron-transfer mechanism at the transition state. At r_x = *ca.* 2.0 Å, the amount of positive charge on the nitrone carbon (C-2) increases and the negative charge on *tert*-butoxyl oxygen also increases. This result indicates that electron transfer definitely occurs from PBN to the *tert*-butoxyl radical. The abrupt change in energy, geometry, spin density and electron density of the spin-trapping system occurs at r_x = 2.0 Å, which suggests that the transition state exists near this point on the reaction co-ordinate.

The steric effect of the substituents on the structure of reactant and product molecules was evaluated further in order to solve the problem of why the cyclohexyl radical could not easily be trapped. The experimental values of the absolute rate constants for carboxyl radical trapping by X-PBN indicated that decarboxylation of cyclohexanecarboxyl radical proceeded more rapidly than that of benzoyloxyl radical. Consequently a larger amount of cyclohexyl radical should be generated than is the case for phenyl-radical generation by decomposition of benzoyloxyl radicals. EPR experiments gave contrary results, showing that a small amount of cyclohexyl spin adducts could be observed only when X-PBNs having electron-withdrawing substituent were used as spin traps. This fact suggests that steric effects may play an important role in the cyclohexyl-radical trapping. Therefore we investigated this problem from the

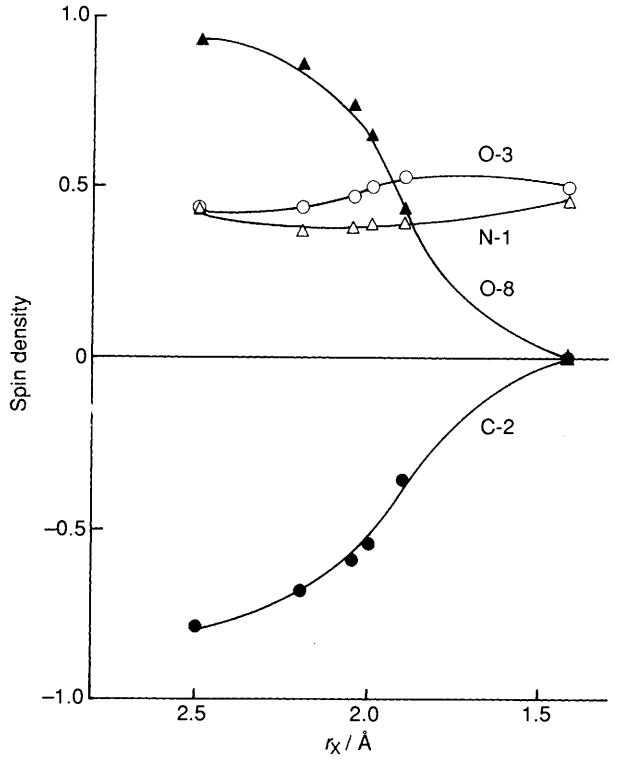

Fig. 3 Spin migration during the process of the spin trapping reaction between *tert*-butoxyl radical and PBN

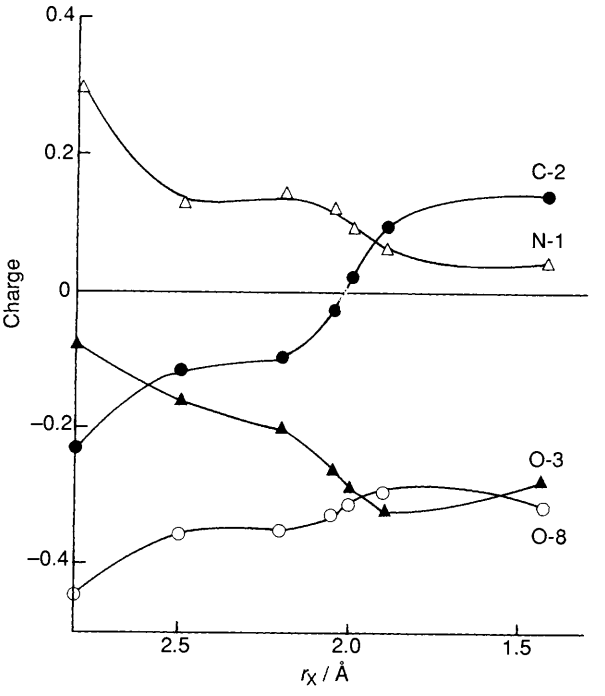

Fig. 4 Change of electron density during the process of the spin trapping reaction between *tert*-butoxyl radical and PBN

viewpoint of the structures of spin adducts. Our MM2 calculations on the phenyl and *tert*-butoxyl PBN spin adducts showed that the phenyl group orients itself *anti* to the *tert*-butyl group in the most predominant conformer (**A**). The conclusion from MM2 was supported by ENDOR and EPR experiments.[19] The stable conformer **A** can be produced easily *via* the reaction pathway proposed in Fig. 2, while conformer **B** cannot be reached directly through the assumed path. In contrast a similar calculation showed that the cyclohexyl group adopts an *anti* position to the *tert*-butyl group in the most stable conformation (**B**) of the cyclohexyl PBN spin adduct. Another conformer corresponding to the most stable conformer **A** of phenyl and *tert*-butoxyl spin adducts was energetically unstable by 5 kcal mol^{-1}.* The instability of this conformer was ascribed to the steric repulsion between *tert*-butyl and cyclohexyl groups. Therefore the trapping of cyclohexyl radical by X-PBN required a larger activation energy than that of phenyl or *tert*-butoxyl radical trapping. In this way, the lower reactivity of cyclohexyl radical towards X-PBNs can reasonably be explained by the steric effects. The cyclohexyl radical is assumed to be consumed through other paths such as dimerization, abstraction of hydrogen from solvents, *etc.* However, such reactions could not be verified because the diamagnetic products of such EPR observable radicals were in amounts too small to be isolated and detected by conventional analytical methods.

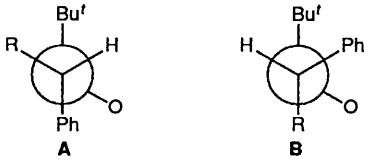

R = Bu^{t}O	most stable	less stable
R = Ph	most stable	less stable
R = *cyclo*-C_6H_{11}	5 kcal mol^{-1} less stable	most stable

* 1 cal = 4.184 J.

Experimental

Preparation of Materials.—Substituted *N*-benzylidene-*tert*-butylamine *N*-oxides (X-PBN) were synthesized from the corresponding substituted benzaldehydes. The aldehydes were reacted with *tert*-butylamine to give *N*-benzylidene-*tert*-butylamines,[20] and the produced imines were oxidized to 3-aryl-2-*tert*-butyloxaziranes[21] by perbenzoic acid. Finally the oxaziranes were thermally isomerized to *N*-oxides by refluxing in acetonitrile.[21] The products were purified by recrystallization and identified by their m.p.s, NMR and mass spectra. *N*-Benzylidene[$^2H_5$]aniline *N*-oxide ([$^2H_5$] DPN) was prepared by the condensation of *N*-[$^2H_5$]phenylhydroxylamine with benzaldehyde. The radical sources were prepared in the following way. Di-*tert*-butyl peroxyoxalate[22] (DBPO) was synthesized by the reaction of *tert*-butyl hydroperoxide with oxalyl chloride. *N*-Acyloxypyridine-2-thiones[23] (Barton's reagent for radical generation) were prepared by treating 1- hydroxypyridine-2-thione[24] with the appropriate acyl chlorides. The synthesized products were characterized by spectroscopy.

Reactions.—Radicals were generated *in situ* by the thermal decomposition of their precursors in solutions at 55 °C. Di-*tert*-butyl peroxyoxalate (DBPO) or *N*-acyloxypyridine-2-thiones (Barton's reagents) were dissolved in pentane 0.03 mol dm^{-3}) or in benzene (0.01 mol dm^{-3}), respectively. The spin-trapping reactions were performed by mixing equal volumes of radical precursor solution and benzene solution (0.01 mol dm^{-3}) of spin trap (X-PBNs or [$^2H_5$]DPN) and heating at 55 °C for 3 min. After the reaction the sample solutions were cooled to liquid nitrogen temperature in order to quench the radical generation. Immediately before the EPR measurement, frozen samples were allowed to stand to melt, and were degassed by bubbling nitrogen gas into the solution.

Measurement of EPR Spectra.—EPR spectra were measured on a JEOL JES-ME-3X spectrometer. Concentrations of the free radicals were determined from the calibration line which was drawn preliminarily by using 4-hydroxy-2,2,6,6-tetramethylpiperidine *N*-oxyl solutions of known concentration, referenced to standard $MnCl_2$ aqueous solutions.

Measurement of Rate Constants by EPR Spectroscopy.—The relative rate constant k_a/k_b was determined on the basis of eqn. (3) by monitoring the amount of the produced X-PBN and [$^2H_5$]DPN spin adducts from EPR spectra at an early stage of the spin trap reaction. Although the EPR peaks of X-PBN and DPN overlap each other considerably, the peaks at the lowest magnetic field end can be observed separately.[5] Thus the intensity of these separated peaks can be used to determine the amount of produced spin adducts. The peak intensities of each pair of spin adducts were measured as the peak-to-trough amplitude. The measurements were repeated 3–5 times with each pair, the average values being used as the observed intensities in order to obtain kinetic data. As the linewidths of the signals were almost the same (0.95–0.97 G) throughout the measurements, the peak-to-trough amplitude could be assumed to be proportional to the concentration of spin adducts. The standard deviations for the peak intensities of the spin adducts were *ca.* 5%.

The rate constants for the elementary processes of the spin trapping reaction in the Barton's reagents system were determined by using eqn. (9). The concentrations of the $RCO_2^{\bullet}$ spin adducts produced were estimated from the peak intensities of EPR spectra as described above.

Measurement of GLC–MS Spectra.—GLC–MS measurements of spin adducts were carried out with Finnigan MAT ITD 800 ion trap detector and Hewlett Packard HP5890 gas chromatograph system. The GLC conditions were as follows: HP DB-1 fused silica capillary column, φ = 0.53 mm, X 30 m, column temp. 100 °C (held 1 min) to 200 °C (at 10 °C min^{-1}), inj. temp. 200 °C. *N,O*-bis(trimethylsilyl)acetamide was used as the trimethylsilylating agent for the spin adducts. Reactions for the trimethylsilylation of spin adducts were carried out in a 1 cm^3 tapered reaction vial sealed with a Teflon-faced rubber disc before the GLC–MS measurements.

Calculations.—Molecular-mechanics calculations were performed by using the MMP2(82) program[25] and semiempirical molecular orbital calculations were carried out with the AM1 program.[26] Calculations were carried out with HITAC M-682H computers at the Computer Centre of the University of Tokyo or with HITAC M-680H computers at the Computer Centre of the Institute for Molecular Science.

Acknowledgements

We would like to thank the Computer Centre, Institute for Molecular Science, Okazaki National Research Institutes for the use of the HITAC M-680H computer for AM1 calculations. We also thank K. Ninomiya (the Yokohama Research Institute for Environmental Protection) for the use of GLC–MS spectrometer. This work was supported by the Grant-in-Aid for Scientific Research on Priority Areas No. 02230101 from the Ministry of Education, Science and Culture, Japanese Government.

References

1 E. G. Janzen, *Acc. Chem. Res.*, 1971, **4**, 31.
2 K. Makino and H. Hatano, *Chem. Lett.*, 1979, 119.
3 K. Abe, H. Suezawa and M. Hirota, *J. Chem. Soc., Perkin Trans. 2*, 1984, 29.
4 D. L. Haire, U. M. Oeher, P. H. Krygsman and E. G. Janzen, *J. Org. Chem.*, 1988, **53**, 4535.
5 K. Murofushi, K. Abe and M. Hirota, *J. Chem. Soc., Perkin Trans. 2*, 1987, 1829.
6 D. H. R. Barton, D. Bridon, Y. Herve and P. Potier, *Tetrahedron*, 1986, **42**, 4983.
7 M. Kamimori, H. Sakuragi, K. Sawatari, T. Suehiro, K. Tokumaru and M. Yoshida, *Bull. Chem. Soc. Jpn.*, 1979, **52**, 2339.
8 C. D. Ritchie and W. F. Sager, *Prog. Phys. Org. Chem.*, 1964, **2**, 223.
9 K. Sommermeyer, W. Seifert and W. Wilker, *Tetrahedron Lett.*, 1974, **20**, 1821.
10 D. F. DeTar, *J. Am. Chem. Soc.*, 1967, **89**, 4058.
11 E. G. Janzen, C. A. Evans and Y. Nishi, *J. Am. Chem. Soc.*, 1972, **94**, 8236.
12 M. J. S. Dewar, E. G. Zoebische, E. F. Healy and J. J. P. Stewart, *J. Am. Chem. Soc.*, 1985, **107**, 3902.
13 N. L. Allinger and H. L. Flanagan, *J. Comput. Chem.*, 1983, **4**, 399.
14 Y. Hase, K. Sakakibara and M. Hirota, *Chem. Lett.*, 1989, 1507.
15 A. E. Dorigo and K. N. Houk, *J. Org. Chem.*, 1988, **53**, 1650.
16 R. P. Johnson, *J. Org. Chem.*, 1984, **49**, 4857.
17 R. V. Lloyd, J. G. Causey and F. A. Momany, *J. Am. Chem. Soc.*, 1980, **102**, 2260.
18 J. Pacansky and D. W. Brown, *J. Phys. Chem.*, 1987, **87**, 1553.
19 E. G. Janzen, U. M. Oehler, D. L. Haire and Y. Kotake, *J. Am. Chem. Soc.*, 1986, **108**, 6856.
20 W. D. Emmons and A. S. Pagano, *Org. Synth.*, Coll. Vol. V, 1973, 191.
21 W. D. Emmons, *J. Am. Chem. Soc.*, 1957, **79**, 5739.
22 P. D. Bartlett and R. E. Pincock, *J. Am. Chem. Soc.*, 1960, **82**, 1962.
23 D. H. R. Barton, H. Togo and S. Z. Zard, *Tetrahedron*, 1985, **41**, 5507.
24 R. A. Jones and A. R. Katritzky, *J. Chem. Soc.*, 1960, 2937.
25 N. L. Allinger, *QCPE*, program No. MMP2(82).
26 M. J. S. Dewar and J. J. P. Stewart, *QCPE*, program No. 523.

Paper 0/04350H
Received 26*th September* 1990
Accepted 18*th December* 1990